Cluster-variation approach to the spin-$\frac{1}{2}$ XXZ model

Dirk Jan Bukman, Guozhong An, and J. M. J. van Leeuwen
Instituut-Lorentz, Rijksuniversiteit te Leiden, P.O. Box 9506, 2300 RA Leiden, The Netherlands
(Received 29 October 1990)

We use the cluster-variation method to examine the phase diagram of the spin-$\frac{1}{2}$ XXZ model. The clusters used consist of two neighboring spins. With this method, we calculate global phase diagrams for arbitrary values of the anisotropy J_z/J and for arbitrary external magnetic fields. Lattices with different values of the coordination number z are considered. Analytic expressions are found for nearly all phase boundaries; the remaining phase boundary is located numerically. Despite some problems at low temperature, the results based on this approach are in quite good agreement with the results from series-expansion methods. A connection is made with the Hubbard model, which can be mapped onto the XXZ Hamiltonian in the limit of strong on-site attraction.

I. INTRODUCTION

Magnetic spin models have been extensively discussed in the literature. Interest in these models derives not only from the need to describe magnetic materials in a simplified way, but also from the fact that certain many-particle systems can be mapped onto such spin models. For instance, simple lattice gas models for classical[1,2] and quantum[3] fluids have been shown to be equivalent to the Ising and XXZ spin models, respectively. Also, the extended Hubbard Hamiltonian can, in the limit of strong attraction, be mapped onto an XXZ spin Hamiltonian.[4,5] Because of the assumed connection between high-T_c superconductivity and the Hubbard model, this has generated renewed interest in these spin models.

In this paper, we will examine the spin-$\frac{1}{2}$ XXZ Hamiltonian

$$\mathcal{H}=-J\sum_{\langle i,j\rangle}(\sigma_i^x\sigma_j^x+\sigma_i^y\sigma_j^y)-J_z\sum_{\langle i,j\rangle}\sigma_i^z\sigma_j^z -h\sum_{i=1}^{N}\sigma_i^z\ . \tag{1.1}$$

The sum $\langle i,j\rangle$ runs over all nearest-neighbor pairs in the N-spin system, and the σ_i^α are Pauli matrices. We will only consider bipartite lattices, thus excluding the possibility of frustration. In that case, the coupling constant J in the x-y plane can always be taken to be positive (i.e., ferromagnetic), because the cases $J>0$ and $J<0$ can be mapped onto each other by a rotation of spins on one sublattice. The coupling constant J_z may assume both positive and negative values.

To make the connection with the extended Hubbard model, we consider a system of electrons moving on a lattice with interactions between electrons both on the same site and on neighboring sites. Its Hamiltonian is given by

$$\mathcal{H}=t\sum_{\langle i,j\rangle,\sigma}(c_{i\sigma}^\dagger c_{j\sigma}+c_{j\sigma}^\dagger c_{i\sigma}) +U\sum_i n_{i\downarrow}n_{i\uparrow}+W\sum_{\langle i,j\rangle,\sigma,\sigma'}n_{i\sigma}n_{j\sigma'} -\mu\sum_{i,\sigma}n_{i\sigma}\ , \tag{1.2}$$

where $c_{i\sigma}^{(\dagger)}$ is the annihilation (creation) operator for an electron of spin σ on site i, while $n_{i\sigma}$ is the number operator $n_{i\sigma}=c_{i\sigma}^\dagger c_{i\sigma}$. The hopping term contains the transfer integral t; the strength of the on-site interaction between the electrons is given by U and of the intersite interaction by W; the number of electrons is controlled by the chemical potential μ.

In the limit of strong on-site attraction, $U=-|U|$ with $|U|\gg t,W$, strongly bound pairs of electrons are formed, and (1.2) can be reduced to a Hamiltonian in which singly occupied sites are excluded.[5] This Hamiltonian can be cast into the form (1.1) as a pseudospin Hamiltonian, and to second order in $t/|U|$, this leads to the following expressions for the coupling constants:

$$J=\frac{t^2}{|U|},\quad J_z=-\frac{t^2}{|U|}-W,\quad h=\mu+\tfrac{1}{2}|U|-zW\ , \tag{1.3}$$

where z is the coordination number of the lattice. The pseudospin operators are then given by

$$\begin{aligned}\sigma_i^x&=c_{i\downarrow}c_{i\uparrow}+c_{i\downarrow}^\dagger c_{i\uparrow}^\dagger\ ,\\ \sigma_i^y&=ic_{i\downarrow}c_{i\uparrow}-ic_{i\downarrow}^\dagger c_{i\uparrow}^\dagger\ ,\\ \sigma_i^z&=n_{i\downarrow}+n_{i\uparrow}-1\ .\end{aligned} \tag{1.4}$$

The last equation implies a relation between the average magnetization and electron density $n_e=\langle n_\downarrow+n_\uparrow\rangle$:

$$n_e=\langle\sigma^z\rangle+1\ . \tag{1.5}$$

There are some special cases of the Hamiltonian (1.1), like the Ising and isotropic Heisenberg models, about which much is known both from analytical results and from approximations of different degrees of sophistication that have been applied to these models. But about the Hamiltonian in its full anisotropic form, far less is known, and practically the only general method dealing with the properties of (1.1) is the mean-field approximation. In the mean-field approximation, the correlations between fluctuations are ignored. In classical spin models, such correlations can be incorporated quite accurately by the cluster-variation method (CVM). The CVM has the intrinsic drawback that it cannot account properly

for the critical fluctuations, but it is quite successful in calculating phase diagrams. Moreover, by use of the coherent-anomaly method, nonclassical critical phenomena can also be incorporated.[6]

We have applied the cluster-variation method to the Hamiltonian (1.1), confining ourselves to its simplest form, which only uses 2-spin clusters. As a first improvement over the mean-field approximation, this already gives significantly different results. It turns out to be possible to derive analytical expressions for the boundaries between most of the phases, while the behavior of the system and location of all phase boundaries can also be examined numerically. The CVM has earlier been applied to this Hamiltonian by Kulik and Pedan.[7] They made, however, additional assumptions on the density matrices which cause their results to be quite different from what we obtain in this paper.

Using the cluster-variation method, we obtain global phase diagrams for arbitrary ratios J_z/J, both ferromagnetic and antiferromagnetic, and for arbitrary fields h. Lattices with different values of the correlation number z are considered. We will examine these phase diagrams both in the context of a spin model and in connection with the Hubbard model, and compare them with the results of other approximations and with exact results where available. Despite the fact that this method behaves unphysically at low temperatures, which makes its results unreliable in some cases, in those cases where this behavior does not interfere with the rest of the phase diagram, its results are quite accurate.

II. CLUSTER-VARIATION METHOD

The basic ingredient of the CVM (Refs. 8 and 9) is the variational principle of statistical mechanics which states that the density matrix describing a system in equilibrium can be found by minimizing the free-energy functional $\mathcal{F}$. This functional has the form

$$\mathcal{F}=\mathrm{Tr}(\rho\mathcal{H})+k_BT\,\mathrm{Tr}(\rho\ln\rho)\ , \tag{2.1}$$

where $\rho=\rho(j_1,\ldots,j_N)$ is a trial density matrix of a system of spins $j_1,\ldots,j_N$ that satisfies the constraint

$$\mathrm{Tr}\rho=1\ . \tag{2.2}$$

The free energy F is then given by

$$\begin{aligned}F&=\min\mathcal{F}=\mathrm{Tr}(\rho_0\mathcal{H})+k_BT\,\mathrm{Tr}(\rho_0\ln\rho_0)\\&=E-TS\ ,\end{aligned} \tag{2.3}$$

where the density matrix that minimizes $\mathcal{F}$ is

$$\rho_0=\frac{e^{-\beta\mathcal{H}}}{\mathrm{Tr}e^{-\beta\mathcal{H}}}\ . \tag{2.4}$$

The advantage of the formulation (2.3) is that one can write $\mathcal{F}$ as an infinite series of terms, each of which corresponds to a cluster containing a certain number of lattice points. One expects the importance of these terms to decrease as the cluster size increases, and an approximation can be made by neglecting all contributions except those corresponding to a limited number of small clusters.

To make an expression for $\mathcal{F}$ in this way, we express it in terms of the reduced density matrices corresponding to the different clusters:

$$\rho^{(n)}_{i_1,\ldots,i_n}\equiv\mathop{\mathrm{Tr}}_{j_1,\ldots,j_{N-n}}\rho(i_1,\ldots,i_n,j_1,\ldots,j_{N-n})\ , \tag{2.5}$$

where all spins except the ones contained in the cluster $i_1,\ldots,i_n$ are traced out. For a Hamiltonian of the form (1.1), which only contains on-site and nearest-neighbor interactions, the first term of (2.1) can be expressed in the reduced density matrices as

$$\mathrm{Tr}(\rho\mathcal{H})=\sum_i\mathrm{Tr}(\rho^{(1)}_i h^{(1)}_i)+\sum_{\langle i,j\rangle}\mathrm{Tr}(\rho^{(2)}_{i,j}h^{(2)}_{i,j})\ , \tag{2.6}$$

where $h^{(1)}_i$ is the on-site interaction of spin i and $h^{(2)}_{i,j}$ is the interaction between spins i and j:

$$\begin{aligned}h^{(1)}_i&=-h\sigma^z_i\ ,\\h^{(2)}_{i,j}&=-J(\sigma^x_i\sigma^x_j+\sigma^y_i\sigma^y_j)-J_z\sigma^z_i\sigma^z_j\ .\end{aligned} \tag{2.7}$$

Now it remains to write the entropy term in (2.1) in terms of the reduced density matrices. A quantity that is convenient from a calculational point of view, as it involves only one reduced density matrix, is the cluster entropy S, defined by

$$S^{(n)}_{j_1,\ldots,j_n}=-k_B\mathrm{Tr}(\rho^{(n)}_{j_1,\ldots,j_n}\ln\rho^{(n)}_{j_1,\ldots,j_n})\ . \tag{2.8}$$

These cluster entropies can be expressed in terms of the so-called cumulants $\tilde{S}$ as follows:

$$S^{(n)}_{j_1,\ldots,j_n}=\sum_i\tilde{S}^{(1)}_i+\sum_{i<j}\tilde{S}^{(2)}_{i,j}+\cdots+\tilde{S}^{(n)}_{j_1,\ldots,j_n}\ . \tag{2.9}$$

These relations implicitly define the $\tilde{S}$, and inverting them gives

$$\begin{aligned}\tilde{S}^{(1)}_i&=S^{(1)}_i\ ,\\\tilde{S}^{(2)}_{i,j}&=S^{(2)}_{i,j}-S^{(1)}_i-S^{(1)}_j\ ,\\&\cdots\ .\end{aligned} \tag{2.10}$$

Since obviously the second term in (2.1) is $-TS^{(N)}$, the functional $\mathcal{F}$ can be written as

$$\begin{aligned}\mathcal{F}&=\mathrm{Tr}(\rho\mathcal{H})+k_BT\,\mathrm{Tr}(\rho\ln\rho)\\&=\sum_i\mathrm{Tr}(\rho^{(1)}_i h^{(1)}_i)+\sum_{\langle i,j\rangle}\mathrm{Tr}(\rho^{(2)}_{i,j}h^{(2)}_{i,j})\\&\quad-T\left[\sum_i\tilde{S}^{(1)}_i+\sum_{i<j}\tilde{S}^{(2)}_{i,j}+\cdots+\tilde{S}^{(N)}_{j_1,\ldots,j_N}\right]\ .\end{aligned} \tag{2.11}$$

This expression is still exact, and an approximation can be made by making an ansatz for the density matrix that in some way truncates the expansion in cumulants. For example, taking all reduced density matrices as products of the 1-spin reduced density matrix $\rho^{(1)}_i$ causes all cumulants except $\tilde{S}^{(1)}$ to vanish and leads to the mean-field approximation. An improved approximation is obtained by also taking into account the 2-spin reduced density matrix $\rho^{(2)}_{i,j}$, where spins i and j are nearest neighbors. This is exact for the energy term in (2.11) and accounts for the correlations between neighboring spins that are included in the term $\tilde{S}^{(2)}_{i,j}$. Higher cumulants in expression (2.11)

are ignored in this approximation, and the entropy term becomes, for a lattice with coordination number z,

$$k_B T \,\mathrm{Tr}(\rho \ln\rho) = -T\left[\sum_i \tilde{S}_i^{(1)} + \sum_{\langle i,j\rangle} \tilde{S}_{i,j}^{(2)}\right] = -T\left[\sum_i (1-z) S_i^{(1)} + \sum_{\langle i,j\rangle} S_{i,j}^{(2)}\right] . \quad (2.12)$$

This is the approximation that we will be using in this paper.

III. TWO-SPIN CLUSTER

To apply the CVM, one has to express the functional $\mathcal{F}$ in terms of variational parameters, which is done by choosing a form for the trial density matrix. For a spin-$\frac{1}{2}$ system, one can always express the reduced density matrices in Pauli spin matrices. The coefficients of these matrices are the variational parameters of the problem. In order to be able to describe antiferromagnetic phases, it is necessary to introduce, for a bipartite lattice, two 1-spin reduced density matrices $\rho_a^{(1)}$ and $\rho_b^{(1)}$, one for each of the two sublattices a and b. The 2-spin reduced density matrix is of course always of the form $\rho_{ab}^{(2)} \equiv \rho^{(2)}$.

Thus one can write

$$\rho_i^{(1)} = \tfrac{1}{2}\{1 + c_i^x \sigma_i^x + c_i^y \sigma_i^y + c_i^z \sigma_i^z\}, \quad \text{for } i = a,b . \quad (3.1)$$

It is easy to see that $c_i^x = \mathrm{Tr}(\rho_i^{(1)} \sigma_i^x) = \langle \sigma_i^x \rangle$, and similarly for c_i^y and c_i^z. Also, expression (3.1) satisfies the constraint (2.2). For $\rho^{(2)}$ we write

$$\rho^{(2)} = \frac{1}{4}\left[1 + \sum_i \sum_{\alpha=x,y,z} c_i^\alpha \sigma_i^\alpha + \sum_{\alpha,\beta=x,y,z} c^{\alpha\beta} \sigma_a^\alpha \sigma_b^\beta\right] , \quad (3.2)$$

with $c^{\alpha\beta} \equiv c_{ab}^{\alpha\beta} = \langle \sigma_a^\alpha \sigma_b^\beta \rangle$. The parameters $c_i^\alpha, c^{\alpha\beta}$ must now be chosen such as to minimize $\mathcal{F}$.

In order to explicitly incorporate the bipartite nature of the lattice, which is of importance in the antiferromagnetic phase, we replace the sublattice magnetizations c_i^z by the total magnetization m,

$$m \equiv \tfrac{1}{2}(c_a^z + c_b^z) , \quad (3.3)$$

and the staggered magnetization $\bar{m}$,

$$\bar{m} \equiv \tfrac{1}{2}(c_a^z - c_b^z) . \quad (3.4)$$

An additional advantage in introducing these parameters is that, instead of viewing them both as variational parameters as one would do when considering a spin model, it is also possible to fix m at an externally prescribed value, which would be desirable from the viewpoint of a Hubbard model with a given electron density [see Eq. (1.5)].

Before giving detailed expressions for the reduced density matrices, we first examine the symmetry aspects of the problem; this is useful both for gaining insight into the behavior one should expect and also into the structure of the matrices ρ. Considering the Hamiltonian (1.1) of the spin system, we find that it has the following symmetries.

$\mathcal{H}$ is symmetric under exchange of the sublattice labels a and b. This translation symmetry will be denoted by T_{ab}.

$\mathcal{H}$ is invariant under rotations of the spins in the x-y plane around the z axis; we will denote this symmetry by R_{xy}.

If the field h is zero, $\mathcal{H}$ is symmetric under a rotation of the spins through an angle π around any axis in the x-y plane. Choosing the line $x = y$ in the plane $z = 0$ for the rotation axis, the result of this spin-flip symmetry is $(\sigma^x, \sigma^y, \sigma^z) \rightarrow (\sigma^y, \sigma^x, -\sigma^z)$. We will denote this symmetry by F.

Last, $\mathcal{H}$ is invariant under a reflection of the spins in any plane containing the z axis. If we take the plane $x = y$ as the mirror plane, then this symmetry operation, which we will call I, is the product of time reversal (which lets $\boldsymbol{\sigma} \rightarrow -\boldsymbol{\sigma}$), a spin flip F as described above, and a rotation R_{xy}. Whereas the first three symmetries all correspond to unitary operators, this one is antiunitary because it contains a time reversal.

The presence or absence of these symmetries can be used to classify the different phases of the system. Since the symmetry of the phase is reflected in the form of the reduced density matrix, it can also be used to reduce the number of independent variational parameters. Namely, the only parameters that can be nonzero are those that correspond to operators that are invariant under the symmetries of the phase. For instance, the disordered phase has the full symmetry of the Hamiltonian, and this requirement causes all but a few parameters in the reduced density matrix to be zero. In the different ordered phases, one (or more) of the symmetries of the Hamiltonian is spontaneously broken, and some of the parameters that were required to be zero by this symmetry assume a nonzero value. The most important of these parameters is, of course, the order parameter of the phase in question, but in general any parameter with the same symmetry can and will become nonzero. Table I displays the operators that are invariant under the symmetries of the Hamiltonian.

We will now list the properties of the phases that constitute the phase diagram.

A. Disordered (D) phase

As can be seen from Table I, the only operators that are invariant under all four symmetries of the Hamiltonian are $\sigma_a^x \sigma_b^x + \sigma_a^y \sigma_b^y$ and $\sigma_a^z \sigma_b^z$. Consequently, the properties of the disordered phase in zero field are fully described by the two parameters c^{xx} ($= c^{yy}$) and c^{zz}. In the case that $h \neq 0$, so that the Hamiltonian is not invariant under the spin flip F, one must add m as a third parameter, since $\sigma_a^z + \sigma_b^z$ is invariant under the remaining three symmetries.

B. Ferromagnetic Ising (FI) phase

In the ferromagnetically ordered Ising phase, the spin-flip symmetry F is spontaneously broken, and so we again have the three parameters c^{xx}, c^{zz}, and m to describe this phase. The difference with the previous case is that, instead of being induced by a field, m is now a spontaneous magnetization, which is the order parameter of this

TABLE I. Operators that are invariant under the symmetries of the Hamiltonian. It is indicated whether the operators are ($\times$) or are not ($-$) invariant under the symmetries mentioned in the text; if two operators are listed together, it is indicated whether each one is conserved individually, or only their sum or difference.

Operators	Symmetries T_{ab}	R_{xy}	F	I
$\sigma_a^x+\sigma_b^x$, $\sigma_a^y+\sigma_b^y$	Each	$-$	Sum	Sum
$\sigma_a^x+\sigma_a^y$, $\sigma_b^x+\sigma_b^y$	Sum	$-$	Each	Each
σ_a^z, σ_b^z	Sum	Each	$-$	Each
$\sigma_a^x\sigma_b^x$,$\sigma_a^y\sigma_b^y$	Each	Sum	Sum	Sum
$\sigma_a^z\sigma_b^z$	$\times$	$\times$	$\times$	$\times$
$\sigma_a^x\sigma_b^y$, $\sigma_a^y\sigma_b^x$	Sum	Diff.	Sum	Sum
$\sigma_a^x\sigma_b^z+\sigma_a^z\sigma_b^x$, $\sigma_a^y\sigma_b^z+\sigma_a^z\sigma_b^y$	Each	$-$	$-$	Sum
$\sigma_a^x\sigma_b^z$, $\sigma_a^y\sigma_b^z$	$-$	$-$	Diff.	Sum
$\sigma_a^z\sigma_b^x$, $\sigma_a^z\sigma_b^y$	$-$	$-$	Diff.	Sum

phase. If the Ising symmetry is absent because of an applied magnetic field h, the phase transition is destroyed.

C. Antiferromagnetic Ising (AI) phase

Breaking of the translational symmetry T_{ab} is characteristic of the antiferromagnetic Ising phase. This implies that, in addition to the three parameters c^{xx}, c^{zz}, and m, the staggered magnetization $\overline{m}$, which is the order parameter of this phase, also becomes nonzero.

D. x-y ordered (XY) phase

If the rotation symmetry R_{xy} is broken, this leads to a phase with a magnetization in the x-y plane. Because of the symmetry in the Hamiltonian between $-J$ and J, this phase can always be taken to be ferromagnetic. We choose the direction of the magnetization such that the order parameter satisfies $c_i^x=c_i^y$, in order to keep the reflection symmetry I in the plane $x=y$ intact. In fact, in whatever way one chooses the direction of this magnetization, there is always a reflection symmetry in the plane containing this direction and the z axis. This symmetry remains unbroken in all ordered phases. Because of the sublattice symmetry, we have $c_a^x=c_b^x=c_a^y=c_b^y\equiv c^x$. Apart from the order parameter, several other parameters become nonzero, once the symmetry R_{xy} is broken, such as $c^{xy}=c^{yx}$, and provided that $h\neq 0$, $c^{xz}=c^{yz}=c^{zx}=c^{zy}$.

E. Mixed (M) phase

A final possibility is the simultaneous breaking of the rotational and sublattice symmetries, which gives rise to the so-called mixed phase. In this phase, the only unbroken symmetry is I, and c_a^x, c_b^x, and $\overline{m}$ all assume distinct values, as well as c^{xy}, c^{xz}, and c^{zx}. This phase can be found as an intermediate phase between the antiferromagnetic Ising and the x-y ordered phases, but only when the extensive quantity m is used as an externally imposed parameter [cf. Eq. (15)]. If one chooses to use the intensive quantity h instead, no mixed phase is found, and in its place we have a first-order transition between the antiferromagnetic Ising and x-y ordered phases, with a discontinuity in the value of m. A summary of the characteristics of these phases can be found in Table II.

Taking into account all parameters that appear in Table II, we obtain the most general form for the reduced density matrices. Writing $\rho_i^{(1)}$ and $\rho^{(2)}$ in the bases $\{|+\rangle,|-\rangle\}$ and $\{|++\rangle,|+-\rangle,|-+\rangle,|--\rangle\}$, respectively, we have

$$\rho_i^{(1)}=\frac{1}{2}\begin{pmatrix} 1+c_i^z & (1-i)c_i^x \\ (1+i)c_i^x & 1-c_i^z \end{pmatrix},$$

$$\rho^{(2)}=\frac{1}{4}\begin{pmatrix} 1+2m+c^{zz} & (1-i)(c_b^x+c^{zx}) & (1-i)(c_a^x+c^{xz}) & -2ic^{xy} \\ (1+i)(c_b^x+c^{zx}) & 1+2\overline{m}-c^{zz} & 2c^{xx} & (1-i)(c_a^x-c^{xz}) \\ (1+i)(c_a^x+c^{xz}) & 2c^{xx} & 1-2\overline{m}-c^{zz} & (1-i)(c_b^x-c^{zx}) \\ 2ic^{xy} & (1+i)(c_a^x-c^{xz}) & (1+i)(c_b^x-c^{zx}) & 1-2m+c^{zz} \end{pmatrix}. \tag{3.5}$$

For the energy part (2.6), this gives

TABLE II. Characteristics of the different phases.

Phase	Order parameter	Other nonzero parameters	Spontaneously broken symmetry
Disordered		c^{xx},c^{zz},m	None
Ferro Ising	m	c^{xx},c^{zz}	F
Antiferro Ising	$\overline{m}$	c^{xx},c^{zz},m	T_{ab}
x-y ordered	c^x	$c^{xx},c^{zz},c^{xy},c^{xz},m$	R_{xy}
Mixed	$c_a^x,\overline{m}$	$c_b^x,c^{xx},c^{zz},c^{xy},c^{xz},c^{zx},m$	R_{xy} and T_{ab}

$$\mathrm{Tr}(\rho\mathcal{H})=\sum_i \mathrm{Tr}(\rho_i^{(1)}h_i^{(1)})+\sum_{\langle i,j\rangle}\mathrm{Tr}(\rho_{ij}^{(2)}h_{ij}^{(2)})=-N(zJc^{xx}+\tfrac{1}{2}zJ_zc^{zz}+mh)\ . \tag{3.6}$$

To calculate the entropy term (2.12),

$$k_BT\,\mathrm{Tr}(\rho\ln\rho)=k_BTN\left[\frac{1-z}{2}\sum_{i=a,b}\mathrm{Tr}(\rho_i^{(1)}\ln\rho_i^{(1)})+\frac{z}{2}\mathrm{Tr}(\rho^{(2)}\ln\rho^{(2)})\right], \tag{3.7}$$

it is necessary to find the eigenvalues of the reduced density matrices.

To find the boundaries between the different phases, it is not necessary to diagonalize the full matrix (3.5). Provided that the phase transition into a phase with x-y order (XY or M) is a continuous one, the parameters characteristic of this order, c_i^x, c^{xz}, c^{zx}, and c^{xy}, will still be small at the onset and zero on the phase boundary. Therefore, it suffices to calculate $\mathcal{F}$ to second order in these parameters. In fact, c^{xy} will be neglected altogether, since near the phase boundary it turns out to be of order $O((c^x)^2)$ and it only enters into $\mathcal{F}$ quadratically, thus giving a fourth-order contribution. Note that this procedure makes it impossible to find the boundary between the XY and M phases analytically, since there c_i^x and the other parameters associated with x-y order are nonzero on both sides of the boundary. We will therefore study this part of the phase diagram numerically.

In order to distinguish between the cases with and without x-y order, we split the reduced density matrices into two parts:

$$\rho=\rho_0+\rho_1\ , \tag{3.8}$$

where ρ_0 is the rotationally invariant part, describing the phases without x-y order (where ρ_1 is zero), and ρ_1 is the part that breaks the rotation symmetry. Therefore, ρ_0 only contains the parameters that are invariant under rotation, m, $\overline{m}$, c^{xx}, and c^{zz}, while ρ_1 contains the parameters that only exist in phases where this symmetry is broken, c_i^x, c^{xy}, c^{xz}, and c^{zx}. Consequently, ρ_1 will be small in comparison with ρ_0 near the boundary of these phases, and we are allowed to treat it as a perturbation to ρ_0 in this region.

Since it is rotationally invariant (commutes with S^z_{tot}), ρ_0 has a block diagonal form, only coupling states with the same eigenvalue for S^z_{tot}. This makes it relatively easy to diagonalize exactly, finding its eigenvalues λ_i^0 and eigenvectors $\mathbf{x}_i$. One can then calculate the free-energy functional $\mathcal{F}$ in terms of the parameters m, $\overline{m}$, c^{xx}, and c^{zz}, using

$$\mathrm{Tr}(\rho\ln\rho)=\sum_i\lambda_i^0\ln\lambda_i^0\ , \tag{3.9}$$

and thus exactly solve the minimization equations throughout the phases D, FI, and AI.

Turning to the phases where rotation symmetry is broken, we must also consider the matrix ρ_1, which does not commute with S^z_{tot}. We use a standard perturbation expansion to calculate the eigenvalues of ρ to second order in ρ_1:

$$\begin{aligned}\lambda_i&=\lambda_i^0+\lambda_i^1+\lambda_i^2+\cdots\\&=\lambda_i^0+\mathbf{x}_i^T\cdot\rho_1\cdot\mathbf{x}_i+\sum_j\frac{\mathbf{x}_i^T\cdot\rho_1\cdot\mathbf{x}_j\,\mathbf{x}_j^T\cdot\rho_1\cdot\mathbf{x}_i}{\lambda_i^0-\lambda_j^0}+\cdots\ .\end{aligned} \tag{3.10}$$

The first-order term λ_i^1 is zero because ρ_1 only couples states with different eigenvalues for S^z_{tot}, while ρ_0 only couples equal values of S^z_{tot}. We are then left with the second-order term, which is bilinear in the parameters c_i^x, c^{xy}, c^{xz}, and c^{zx}. To second order in these parameters, the traces in (3.7) are

$$\begin{aligned}\mathrm{Tr}(\rho\ln\rho)&=\sum_i\lambda_i^0\ln\lambda_i^0+\lambda_i^2\ln\lambda_i^0+\lambda_i^2\\&=\sum_i(\lambda_i^0+\lambda_i^2)\ln\lambda_i^0\ .\end{aligned} \tag{3.11}$$

The last equality holds because $\mathrm{Tr}\rho=\sum_i\lambda_i^0=1$, and so $\sum_i\lambda_i^2=0$.

We will now compute the eigenvalues of the matrices (3.5) in this way. For $\rho_i^{(1)}$ we find, for the unperturbed eigenvalues,

$$\begin{aligned}&\mu_{a1}^0=\tfrac{1}{2}(1+m+\overline{m}),\quad \mu_{b1}^0=\tfrac{1}{2}(1+m-\overline{m})\ ,\\&\mu_{a2}^0=\tfrac{1}{2}(1-m-\overline{m}),\quad \mu_{b2}^0=\tfrac{1}{2}(1-m+\overline{m})\ .\end{aligned} \tag{3.12}$$

The second-order corrections to this are

$$\begin{aligned}&\mu_{a1}^2=\frac{c_a^{x2}}{2(m+\overline{m})},\quad \mu_{b1}^2=\frac{c_b^{x2}}{2(m-\overline{m})}\ ,\\&\mu_{a2}^2=-\frac{c_a^{x2}}{2(m+\overline{m})},\quad \mu_{b2}^2=-\frac{c_b^{x2}}{2(m-\overline{m})}\ .\end{aligned} \tag{3.13}$$

Consequently

$$\begin{aligned}\sum_{i=a,b}\mathrm{Tr}(\rho_i^{(1)}\ln\rho_i^{(1)})=\frac{1}{2}\Bigg[&(1+m+\overline{m})\ln(1+m+\overline{m})+(1-m-\overline{m})\ln(1-m-\overline{m})+(1+m-\overline{m})\ln(1+m-\overline{m})\\&+(1-m+\overline{m})\ln(1-m+\overline{m})-4\ln 2+\frac{c_a^{x2}}{m+\overline{m}}\ln\left[\frac{1+m+\overline{m}}{1-m-\overline{m}}\right]\\&+\frac{c_b^{x2}}{m-\overline{m}}\ln\left[\frac{1+m-\overline{m}}{1-m+\overline{m}}\right]\Bigg]+\text{higher-order terms}\ .\end{aligned} \tag{3.14}$$

Proceeding analogously for $\rho^{(2)}$, we find

$$\lambda_1^0=\tfrac{1}{4}(1+2m+c^{zz})\ ,\ \lambda_2^0=\tfrac{1}{4}\left[1+2\overline{m}\left[1+\frac{c^{xx2}}{\overline{m}^{\,2}}\right]^{1/2}-c^{zz}\right],$$
$$\lambda_3^0=\frac{1}{4}\left[1-2\overline{m}\left[1+\frac{c^{xx2}}{\overline{m}^{\,2}}\right]^{1/2}-c^{zz}\right],\ \lambda_4^0=\tfrac{1}{4}(1-2m+c^{zz})\ . \tag{3.15}$$

The second-order terms are

$$\lambda_i^2=\frac{1}{8(1+\xi^2)}\left[\frac{P_{ij}}{\lambda_i^0-\lambda_j^0}+\frac{P_{ik}}{\lambda_i^0-\lambda_k^0}\right], \tag{3.16}$$

with $j=2$ and $k=3$ for $i=1$ and 4, and $j=1$ and $k=4$ for $i=2$ and 3, and where ξ is defined by

$$\xi\equiv\frac{\overline{m}}{c^{xx}}\left[\left[1+\frac{c^{xx2}}{\overline{m}^{\,2}}\right]^{1/2}-1\right]. \tag{3.17}$$

The P_{ij} are given by

$$P_{12}=P_{21}=[c_b^x+c^{zx}+\xi(c_a^x+c^{xz})]^2\ ,\ P_{13}=P_{31}=[c_a^x+c^{xz}-\xi(c_b^x+c^{zx})]^2\ ,$$
$$P_{24}=P_{42}=[c_a^x-c^{xz}+\xi(c_b^x-c^{zx})]^2\ ,\ P_{34}=P_{43}=[c_b^x-c^{zx}-\xi(c_a^x-c^{xz})]^2\ . \tag{3.18}$$

Then we have, for the last term in (3.7),

$$\mathrm{Tr}(\rho^{(2)}\ln\rho^{(2)})=\sum_{i=1}^{4}\lambda_i^0\ln\lambda_i^0+\frac{1}{2(1+\xi^2)}\{P_{12}l_{12}+P_{13}l_{13}+P_{24}l_{24}+P_{34}l_{34}\}+\text{ higher-order terms }, \tag{3.19}$$

where

$$l_{ij}\equiv\frac{\ln(\lambda_i^0/\lambda_j^0)}{4(\lambda_i^0-\lambda_j^0)}\ . \tag{3.20}$$

IV. MINIMIZATION OF $\mathcal{F}$

Collecting all information from the previous sections and scaling $\mathcal{F}$ with Nk_BT, we find, for the functional to be minimized,

$$\Phi\equiv\frac{\mathcal{F}}{Nk_BT}=-z(Kc^{xx}+\tfrac{1}{2}K_zc^{zz})-mH+\tfrac{1}{2}(1-z)\sum_{i=a,b}\mathrm{Tr}(\rho_i^{(1)}\ln\rho_i^{(1)})+\tfrac{1}{2}z\mathrm{Tr}(\rho^{(2)}\ln\rho^{(2)})\ , \tag{4.1}$$

where

$$K=\frac{J}{k_BT},\ K_z=\frac{J_z}{k_BT},\ H=\frac{h}{k_BT}\ . \tag{4.2}$$

A. Phases without *x-y* order

We will first consider the phases which do not have *x-y* order (*D*, FI, and AI). In these phases, the parameters c_i^x, c^{xz}, and c^{zx} are zero, and we only need to take into account the terms in (3.14) and (3.19) that are due to ρ_0. This leads to an expression for Φ that only involves the unperturbed eigenvalues: $\Phi=\Phi_0$. The minimization can then be done exactly, and we find expressions describing the behavior of the system throughout these phases.

Minimizing Φ_0 with respect to the four relevant parameters, we find

$$\frac{\partial\Phi_0}{\partial c^{xx}}=-zK+\frac{zc^{xx}}{4\overline{m}}\left[1+\frac{c^{xx2}}{\overline{m}^{\,2}}\right]^{-1/2}\ln\left[\frac{\lambda_2^0}{\lambda_3^0}\right]=0\ , \tag{4.3}$$

$$\frac{\partial\Phi_0}{\partial c^{zz}}=-\frac{z}{2}K_z+\frac{z}{8}\ln\left[\frac{\lambda_1^0\lambda_4^0}{\lambda_2^0\lambda_3^0}\right]=0\ , \tag{4.4}$$

$$\frac{\partial\Phi_0}{\partial m}=-H+\frac{1-z}{4}\ln\left[\frac{(1+m+\bar{m})(1+m-\bar{m})}{(1-m+\bar{m})(1-m-\bar{m})}\right]+\frac{z}{4}\ln\left[\frac{\lambda_1^0}{\lambda_4^0}\right]=0\ , \tag{4.5}$$

$$\frac{\partial\Phi_0}{\partial\bar{m}}=\frac{1-z}{4}\ln\left[\frac{(1+m+\bar{m})(1-m+\bar{m})}{(1+m-\bar{m})(1-m-\bar{m})}\right]+\frac{z}{4}\left[1+\frac{c^{xx2}}{\bar{m}^2}\right]^{-1/2}\ln\left[\frac{\lambda_2^0}{\lambda_3^0}\right]=0\ . \tag{4.6}$$

We will now apply these equations to the three phases D, FI, and AI.

1. Disordered phase

In the disordered phase we can set $\bar{m}=0$ in Eqs. (4.3)–(4.5), while (4.6) does not apply. From (4.3) and (4.4), we then find

$$4K=\ln\left[\frac{1+2c^{xx}-c^{zz}}{1-2c^{xx}-c^{zz}}\right]\ , \tag{4.7}$$

$$4K_z=\ln\left[\frac{(1+2m+c^{zz})(1-2m+c^{zz})}{(1+2c^{xx}-c^{zz})(1-2c^{xx}-c^{zz})}\right]\ . \tag{4.8}$$

It follows from (4.7) that

$$2c^{xx}=(1-c^{zz})\tanh(2K)\ . \tag{4.9}$$

Defining $\sigma=e^{4K_z}$, (4.8) reduces to

$$\sigma=\frac{(1+2m+c^{zz})(1-2m+c^{zz})}{(1+2c^{xx}-c^{zz})(1-2c^{xx}-c^{zz})}\ , \tag{4.10}$$

and combined with (4.9) this gives an expression for c^{zz}:

$$c^{zz}=\frac{\sigma+\theta-2[\sigma\theta+m^2(\theta^2-\sigma\theta)]^{1/2}}{\sigma-\theta}\ , \tag{4.11}$$

where we have defined $\theta\equiv\cosh^2(2K)$.

From (4.5), we find

$$4H=2(1-z)\ln\left[\frac{1+m}{1-m}\right]+z\ln\left[\frac{1+2m+c^{zz}}{1-2m+c^{zz}}\right]\ . \tag{4.12}$$

Combined with (4.11), this gives m implicitly for given values of K, K_z, and H, or when m is viewed as an externally controlled parameter (like the electron density in the Hubbard model), it gives the field (or the chemical potential in the Hubbard model) that is required to obtain a certain value for m.

These equations completely determine the parameters that play a role in the disordered phase. Next, we will consider the two Ising ordered phases.

2. Ferromagnetic Ising phase

If the external field H is zero, m is the order parameter for the ferromagnetically ordered Ising phase, which does not exist outside the $H=0$ plane. Putting the field equal to zero in (4.12), one finds, to first order in m,

$$m\left[1-z+\frac{z}{1+c^{zz}}\right]=0\ . \tag{4.13}$$

The solution $m=0$ corresponds to the high-temperature phase and the point where the expression in brackets becomes zero, allowing a nonzero value for m, signals the onset of the ordered phase. The phase boundary is thus given by

$$c^{zz}=\frac{1}{z-1}\ . \tag{4.14}$$

On the other hand, on the boundary with the disordered phase c^{zz} is also given by (4.11), and m is zero by continuity. Then (4.11) reduces to

$$c^{zz}=\frac{e^{2K_z}-\cosh(2K)}{e^{2K_z}+\cosh(2K)}\ . \tag{4.15}$$

From (4.14) and (4.15), the equation for the boundary of the ferromagnetic Ising phase is found to be

$$K_z=\frac{1}{2}\left[\ln\left[\frac{z}{z-2}\right]+\ln\cosh(2K)\right]\ . \tag{4.16}$$

3. Antiferromagnetic Ising phase

To examine the antiferromagnetic Ising phase, one also needs to take the staggered magnetization into account. Thus one needs all four Eqs. (4.3)–(4.6) to describe this phase. An expression giving the phase boundary can be found by combining (4.3) and (4.6) to give

$$c^{xx}=\frac{4zK}{z-1}\bar{m}\left[\ln\left[\frac{(1+m+\bar{m})(1-m+\bar{m})}{(1+m-\bar{m})(1-m-\bar{m})}\right]\right]^{-1}\ . \tag{4.17}$$

Then, taking the limit $\bar{m}\to 0$, this is

$$c^{xx}=\frac{1-m^2}{z-1}zK\ . \tag{4.18}$$

For $\bar{m}=0$, we can also use (4.9) and (4.11), and together these three equations determine the boundary of the antiferromagnetic Ising phase.

B. Phases with x-y order

For the phases that do have x-y order (XY and M), we use the perturbation expansion (3.10), and so we can only find the boundaries where the order vanishes. As can be seen from (3.14) and (3.19), Φ now consists of the unperturbed term Φ_0, plus a term due to the inclusion of ρ_1 to

second order, which is bilinear in c_i^x, c^{xz}, and c^{zx}. So we can write $\Phi=\Phi_0+\mathbf{c}^T\Phi_2\mathbf{c}$, where the vector $\mathbf{c}$ is $(c_a^x,c_b^x,c^{xz},c^{zx})^T$ and Φ_2 is a symmetric 4×4 matrix. Taking the derivative with respect to the parameters $\mathbf{c}$ then leads to the matrix equation $\Phi_2\mathbf{c}=\mathbf{0}$. The trivial solution $\mathbf{c}=\mathbf{0}$ is valid in the phases without x-y order and the point where $\det\Phi_2=0$, which allows a nonzero solution for $\mathbf{c}$, indicates the phase boundary.

1. *x-y ordered phase*

First, considering the x-y ordered phase, the matrix Φ_2 can be simplified by using the sublattice symmetry, which is still unbroken in this phase. This allows us to set $\bar{m}=0$, which implies $\xi=1$ [where we take $\bar{m}\downarrow0$ in (3.17)]. Also, of the four parameters in $\mathbf{c}$, only two are independent: $c_a^x=c_b^x$ and $c^{xz}=c^{zx}$. We are then left with a (2×2) determinant:

$$\det\Phi_2=\begin{vmatrix} \frac{1-z}{2m}\ln\left[\frac{1+m}{1-m}\right]+\frac{z}{2}(l_{12}+l_{24}) & \frac{z}{2}(l_{12}-l_{24}) \\ \frac{z}{2}(l_{12}-l_{24}) & \frac{z}{2}(l_{12}+l_{24}) \end{vmatrix}=0\ , \tag{4.19}$$

where the l_{ij} are defined in (3.20). This leads to the following equation:

$$\frac{1-z}{m}\ln\left[\frac{1+m}{1-m}\right]+4z\frac{l_{12}l_{24}}{l_{12}+l_{24}}=0\ . \tag{4.20}$$

By substituting (4.9) and (4.11) into this equation, one can find the boundary between the disordered and x-y ordered phases.

2. *Mixed phase*

In the mixed phase, the sublattice symmetry is also broken. Consequently, $\bar{m}$ is not zero, while we have four independent parameters in $\mathbf{c}$: c_a^x, c_b^x, c^{xz}, and c^{zx}. This means that we have to solve the full (4×4) determinant $\det\Phi_2$. The expression one finds for Φ_2, as well as the equation it leads to, is rather cumbersome and unenlightening, which is why it has been moved to the Appendix. Still, the equation $\det\Phi_2=0$ in combination with Eqs. (4.3)–(4.6), which hold in the AI phase, does give an analytic expression for the boundary between the antiferromagnetic Ising and mixed phases.

In contrast, the boundary between the mixed and x-y ordered phases cannot be found within our approximation. This is due to the fact that on both sides of this line the parameters c_a^x, c_b^x, c^{xz}, and c^{zx} are nonzero; nor are they small in this region. Therefore, the expansion (3.10) is not valid here. Nevertheless, to get an idea of the location of the boundary, we used a numerical algorithm. This algorithm minimizes Φ as a function of the full set of parameters as they are included in (3.5). The results of this algorithm were also used as a check on the analytical calculations in the preceding sections.

Our method treats all clusters as equivalent; therefore, the magnetization m is constant throughout the system. Thus the mixed phase is stable when one insists on a homogeneous magnetization. This need not be so when the system is allowed to phase separate into regions with different values of m. The mixed phase disappears when one does not choose a fixed value for m, but fixes the field H instead, leaving m as a free variational parameter. It collapses onto a single line, forming a first-order transition between the AI and XY phases, with m changing discontinuously across this line.

V. RESULTS

Using the results of Sec. IV, we can now construct phase diagrams for different values of z. We will first discuss the significant features of one specific example, which is more or less representative for the general case. After that, we will point out the differences and similarities with other phase diagrams. We start by considering the case $z=6$, which corresponds to a simple cubic lattice (note that the plane triangular lattice, which also has $z=6$, is not bipartite, and thus does not fall within the scope of our treatment). The phase diagram should of course be considered in a three-dimensional space, as a function of K, K_z, and H. But we will first look at the plane $H=0$ and later consider what happens as a magnetic field is turned on.

In Fig. 1 we have plotted the three curves corresponding to Eq. (4.16), (4.18), and (4.20). These equations are only valid for the boundaries between the ordered phases (FI, AI, and XY), on the one hand, and the disordered phase (D) on the other hand. Therefore, only certain segments of the curves (the solid curves in Fig. 1) have physical relevance. They represent second-order transitions between the ordered phases and the disordered phase. Their location should be compared to the mean-field approximation, which gives $K_c=K_{zc}=1/z$ (the dotted box in Fig. 1), and to the results from series expansions for certain special ratios of K and K_z (the circled crosses in the figure).[10–12] The results of the CVM turn out to be in quite good agreement with the series-expansion values, and in any case they are a substantial improvement over the mean-field approximation. For some special cases, like the ferromagnetic and antiferromagnetic Ising and Heisenberg models, our results agree with those of earlier calculations with the CVM,[13] and of the constant coupling method,[14] which can be shown to be equivalent to our method.

As for the boundaries between the ordered phases, they do not follow from Eqs. (4.16), (4.18), and (4.20). If $H=0$, it is obvious from symmetry considerations that

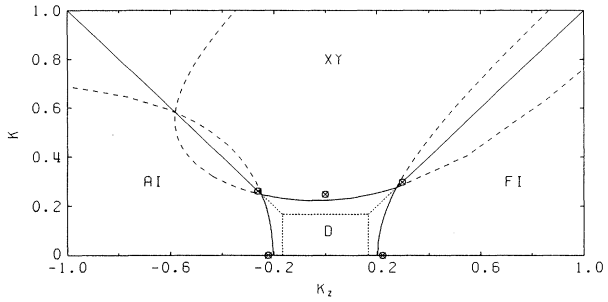

FIG. 1. Phase diagram for $z=6$ and $H=0$. The phase boundaries according to the CVM are indicated by continuous lines. The dashed lines are those parts of the curves calculated in Sec. IV that do not correspond to a phase transition. The dotted lines are the phase boundaries as they are given by the mean-field approximation. The circled crosses show the location of the phase transition for some special cases according to series-expansion calculations.

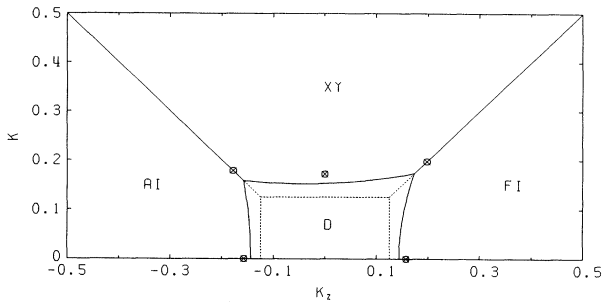

FIG. 2. Phase diagram for $z=8$ and $H=0$. The same description applies as given for Fig. 1. Those parts of the curves that do not correspond to a phase transition (dashed in Fig. 1) are omitted for clarity; they look qualitatively the same as in Fig. 1.

the AI-XY boundary lies on the line $K_z=-K$. The FI-XY boundary only exists for $H=0$, and, again for symmetry reasons, it is immediately evident that it must lie on the line $K_z=K$. Thus the sections of the curves (dashed in Fig. 1) that extend across those lines into a different ordered phase, like the part of the XY curve that lies inside the AI phase, have no physical relevance, because the equations that describe them do not apply inside the ordered phases.

However, the same can not be said about the parts of the XY and AI boundaries that curve back after crossing the line $K_z=-K$ for a second time (also dashed in Fig. 1). These curves again represent a continuous phase transition between the ordered and disordered phases. This implies that the system, after entering the ordered phase at a certain temperature T_c, becomes disordered again at a lower temperature T_c' and remains so down to $T=0$. This artifact of the approximation was already noted by Kasteleyn and van Kranendonk for the Heisenberg antiferromagnet.[14] It indicates that the 2-spin CVM approach fails at low temperature, possibly because the nearest-neighbor correlations it takes into account are too short ranged to describe long-wavelength spin waves, which play a role at low T.[15] Nevertheless, as long as one can make a clear distinction between the high-temperature range, where the results of the approximation are acceptable, and the low-temperature region, where the unphysical disordering takes place, this method is still a useful approach for obtaining phase diagrams. From Fig. 1 one would conclude that this is indeed the case for $z=6$ and $H=0$.

Turning to higher values of z, we see that Fig. 2, which is for $z=8$ (a bcc lattice) and $H=0$, presents essentially the same features as the previous one. The irrelevant and unphysical parts of the curves have been omitted for clarity; they are qualitatively the same as for $z=6$. Again, the 2-spin CVM is a substantial improvement over the mean-field approximation where the boundary of the disordered phase is concerned and the unphysical disordered phase (not shown in the figure) lies at sufficiently low T. If z is increased further, the results of our method become more and more like the mean-field ones, which are exact for $z=\infty$.

Lowering z, we see that the case $z=4$, for the two-dimensional square lattice, presents a different picture (Fig. 3). The part with $K_z>0$ is acceptable, with the ferromagnetic Heisenberg transition shifted to $K=\infty$, as it should be. But the region with $K_z<0$ seems rather problematic. A gap has opened around the line $K_z=-K$, connecting the "physical" disordered phase at high T with the "unphysical" one at low T. This makes it impossible to clearly distinguish between the high-temperature region where the approximation is valid and the low-temperature regime where it fails. Hence one does not know how to interpret this part of the phase diagram for $z=4$, and it seems that the limit of applicability of the approximation has been reached.

We will now consider the changes in the phase diagram when a magnetic field H is turned on. We will only consider the case $z=6$, as it is representative for other values of z as well. Figure 4 shows four cross sections of the

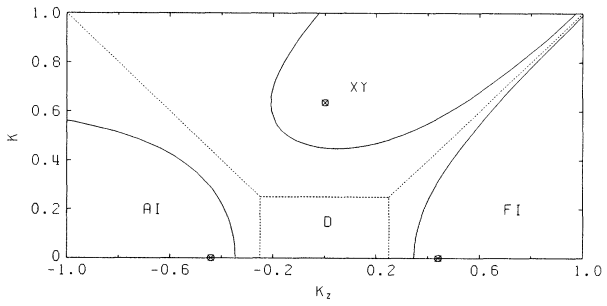

FIG. 3. Phase diagram for $z=4$ and $H=0$. Again, the description given for Fig. 1 applies. In this case the curves calculated in Sec. IV have been entirely drawn as continuous lines, since it is impossible to divide them into real and unphysical phase boundaries in a meaningful way.

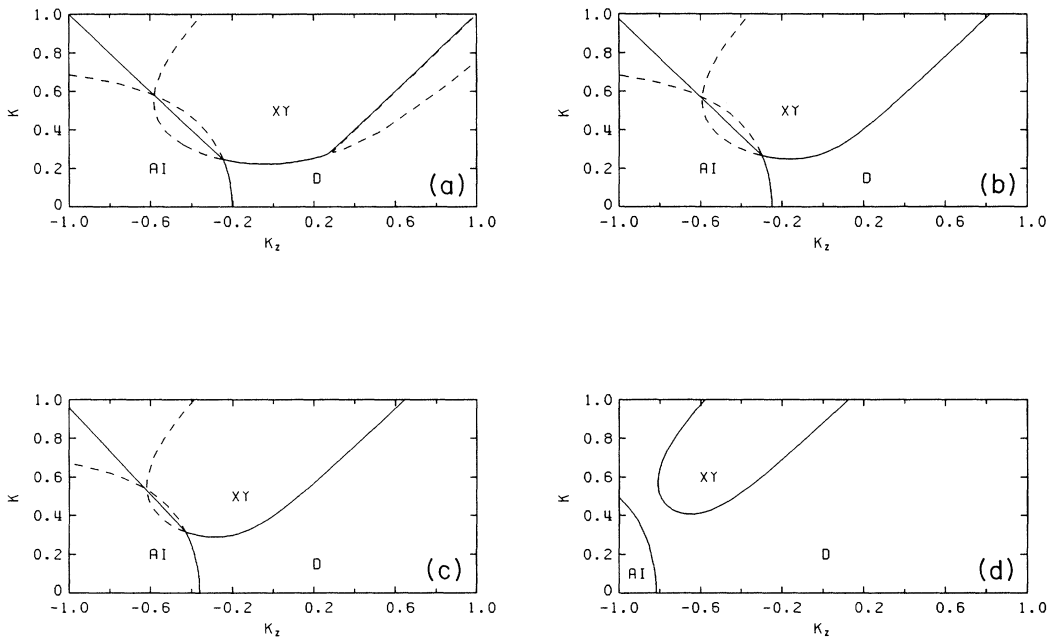

FIG. 4. Phase diagrams for $z=6$ and various values of H. The same description applies as for the previous figures. (a) $H=0.01$, (b) $H=1$, (c) $H=2$, and (d) $H=5$.

three-dimensional phase diagram (containing K, K_z, and H) at certain values of H. The first thing that happens as soon as one turns on a field is the disappearance of the FI phase [Fig. 4(a), where $H=0.01$]. The transition in the ferromagnetic Heisenberg model is also destroyed. The curve giving the XY phase boundary, which for $H=0$ crosses the line $K_z=K$ at the critical coupling for the Heisenberg model, is now split into two separate parts on different sides of this line. The part where $K>K_z$ still indicates the XY phase boundary, which now runs very close to the line $K_z=K$, while the part with $K_z>K$ is irrelevant and does not indicate a phase boundary. The remainder of the figure is not perceptibly changed by the small field $H=0.01$.

On increasing H some trends become apparent [Figs. 4(b)–4(d)]. The XY boundary shifts away from the line $K_z=K$, while the irrelevant part on the other side of this line moves to higher and higher K values, and disappears from the figure. In the other half of the phase diagram, we see that the boundary of the AI phase is shifted toward larger values of $|K_z|$ and also changes in shape slightly. Combined with the narrowing of the XY region, this leads to a shift in the boundary between the XY and AI phases, which leaves the line $K_z=-K$, where it was

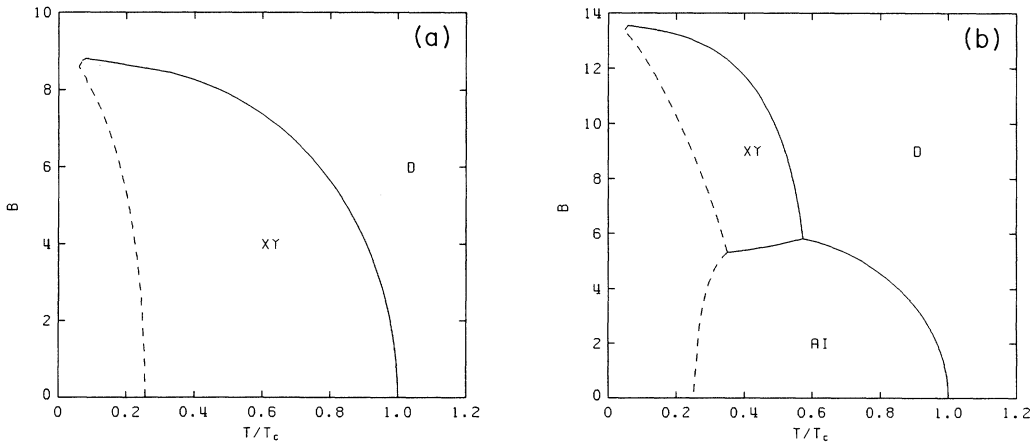

FIG. 5. Phase diagrams for $z=6$ and two different values of the anisotropy J_z/J. Plotted vertically is the magnetic field scaled by the x-y coupling constant, $B=h/J$. The solid lines again indicate the phase boundaries and the dashed lines the unphysical disordering at low T. (a) $J_z=-J/2$ and (b) $J_z=-1.3J$.

located for $H=0$, and moves into the region $-K_z > K$. This phase boundary now becomes first order, with m changing discontinuously when it is crossed. If the field is increased still further, the XY and AI boundaries no longer intersect [Fig. 4(d)], and the same situation arises described earlier for $z=4$ and $H=0$. Again, the approximation ceases to be valid beyond this point.

Another conventional way of drawing the phase diagram of a magnetic system is presented in Fig. 5. Here we have fixed the anisotropy J_z/J and then plot $T/T_c = K_c/K$ versus the scaled field $B = h/J = H/K$ (we again take $z=6$). If the x-y coupling is predominant, the picture is rather simple [Fig. 5(a), where $J_z = -J/2$]. One finds the boundary between the disordered and x-y ordered phases, with a critical temperature that decreases with increasing field, and at lower T the "unphysical" transition back into the disordered phase. A more interesting result is obtained for a model where the z coupling dominates [Fig 5(b), $J_z = -1.3J$]. For low fields B, there is an antiferromagnetically ordered phase, while for higher fields x-y order takes over. These two phases are separated by a first-order transition. At low T, there is again a return to the disordered phase.

Finally, we replot the data in a way appropriate for the Hubbard model. As was pointed out earlier, the externally imposed parameter in the Hubbard model is m, corresponding to the electron density $n_e = m+1$ [see Eq. (1.5)], instead of the field. This leads to the possibility of finding the mixed phase M in place of the first-order transition between the AI and XY phases. Figure 6 shows the phase diagrams for different ratios J_z/J, and again we have taken $z=6$. The phase diagrams are symmetric around $n_e=1$, because of the up-down symmetry in the spin model. In Fig. 6 we only show the half with $n_e > 1$. The region around $n_e=1$ is an AI phase, which in this context is associated with a charge ordered (CO) phase [for $-J_z > J$ one sees from Eq. (1.3) that the intersite interaction W is repulsive; in the charge ordered phase, the electron density is distributed unevenly among the two sublattices so as to minimize the energy due to this repulsion]. This phase is flanked by an XY phase, associated with the superconducting (SC) phase of the Hubbard model. In Fig. 6 a there is a thin slice of the mixed phase in between these two phases, exhibiting both charge order and superconducting order. The boundary between the phases M and SC has been calculated with the numerical procedure mentioned in Sec. IV B 2. For larger values of $|J_z/J|$, the two phases become disconnected, and the mixed phase disappears. This is again an example of the limitations of the approximation, since the unphysical phase at low T links up with the high-T part of the phase diagram.

VI. DISCUSSION

We have applied the cluster-variation method to the spin-$\frac{1}{2}$ XXZ model, using clusters containing two spins. For the phases without x-y order, we have derived the equations that follow from minimizing the free-energy functional. These equations describe the behavior of the system in the disordered and the (anti)ferromagnetic Ising phases, and give analytic expressions for the boundaries between these phases. For the phases with x-y order, we have made an expansion in the parameters that are associated with this order. This makes it possible also to find analytic expressions for the boundaries between phases with and without x-y order. To examine the behavior of the system inside the x-y ordered phases and to find the boundary between phases that both have x-y order, a numerical algorithm was used that performs a minimization of the free-energy functional without any further approximation.

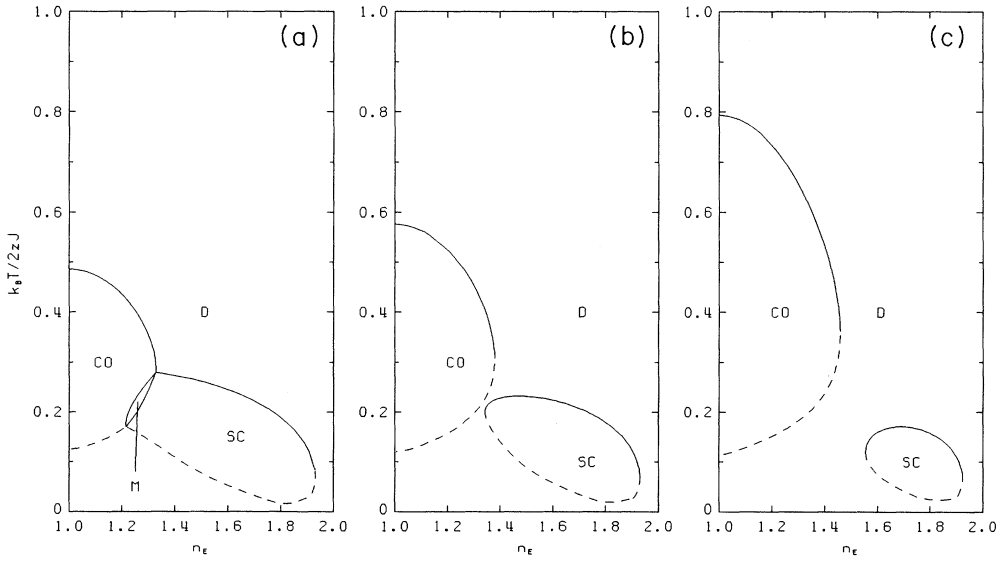

FIG. 6. In the context of the Hubbard model, phase diagrams are usually plotted as a function of the electron density $n_e = m+1$ and temperature. Three different ratios J_z/J are considered, all at $z=6$. The phases CO and SC correspond to the AI and XY phases, respectively, in the spin model. (a) $J_z = -1.3J$, (b) $J_z = -1.5J$, and (c) $J_z = -2J$.

As was mentioned in the Introduction, Kulik and Pedan[7] have also studied some of the properties of a Hamiltonian equivalent to (1.1) with the CVM. But instead of considering both c^{xx} $(=\langle\sigma_a^x\sigma_b^x\rangle)$ and c^{zz} $(=\langle\sigma_a^z\sigma_b^z\rangle)$ as independent variational parameters in the free-energy functional $\mathcal{F}$, they make the assumption

$$c^{xx}\propto c^{x2}\ , \tag{6.1}$$

while keeping c^{zz} as an independent parameter. This assumption does not seem to be justified, since one would expect that for any finite, nonzero temperature there exists a correlation between both the x and z components of neighboring spins, even if the magnetization $c_i^x=\langle\sigma_i^x\rangle$ is zero. Indeed, it can be seen from Eqs. (4.9) and (4.11) that in the disordered phase c^{xx} as well as c^{zz} will be of $O(1)$. Especially near the XY phase boundary, the correlation c^{xx} will be considerable, while the magnetization c_i^x is still zero. As can be seen from Fig. 7, the result of incorporating the mean-field-like assumption (6.1) into the CVM is that the phase diagram (dashed curves) becomes an interpolation between the results of the mean-field approximation (dotted lines) and the full cluster-variation method (solid curves). Some of the important features of the full CVM result (asymmetry between positive and negative K_z, the fact that the FI and AI phase boundaries meet the XY boundary on the lines $K_z=\pm K$) are lost by making the assumption (6.1). Thus it is essential to include both c^{zz} and c^{xx} as independent parameters in a CVM description of a spin model like the one discussed here.

The phase diagrams calculated with the full cluster-variation method are, for a certain range of parameters ($z\geq 6$, H not too large), a substantial improvement over the mean-field approximation and agree quite well with the results from series-expansion methods. The cluster variation method does behave unphysically at low temperatures, predicting a second disordered phase below the ordered phases, but for this range of parameters this does not interfere with the high-temperature part of the phase diagram.

However, for $z\leq 4$ and/or large values of H, the disordered phase at low T links up with the one at high T.

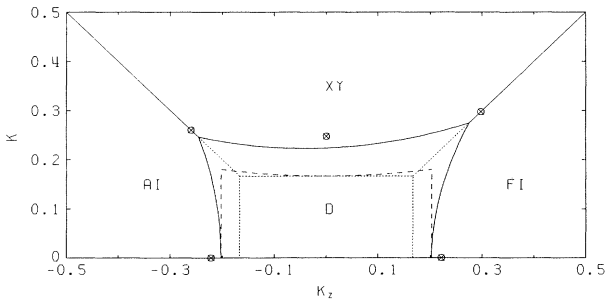

FIG. 7. Comparison between the CVM results with and without assumption (6.1). The phase boundaries shown in Fig. 1 are reproduced, and again we have $z=6$ and $H=0$. The solid lines are the result of the full CVM and the dotted lines those of the mean-field approximation. The dashed lines that form an interpolation between these two are the result of incorporating assumption (6.1) into the CVM.

This makes the phase diagram calculated with our method unreliable in some regions, especially around $J_z=-J$. Other methods that have been used to study the phase diagram of the XXZ model also suffer from this difficulty in dealing with the antiferromagnetic sector. Some real-space renormalization-group approaches that work well for the ferromagnetic Ising sector and the isotropic Heisenberg model turn out to be unable to deal with the rest of the phase diagram in an acceptable manner.[16,17] Despite its shortcomings, the full cluster-variation method seems to be a useful tool to examine the phase diagram of the XXZ model. It is considerably more sophisticated than the mean-field approximation and gives qualitatively better and quite accurate results over a range of parameters.

ACKNOWLEDGMENTS

Part of this research was supported by the Stichting voor Fundamenteel Onderzoek der Materie (FOM), which is financially supported by the Stichting Nederlands Wetenschappelijk Onderzoek (NWO).

APPENDIX

As was pointed out in Sec. IV B 2, to find the boundary separating the AI and M phases, one needs to take into account all four parameters c_a^x, c_b^x, c^{xz}, and c^{zx}. Then one finds the following expression for $\det\Phi_2$:

$$\det\Phi_2=\begin{vmatrix} Q_1+A_1 & C_1 & A_2 & C_2 \\ C_1 & Q_2+\overline{A}_1 & C_2 & \overline{A}_2 \\ A_2 & C_2 & A_1 & C_1 \\ C_2 & \overline{A}_2 & C_1 & \overline{A}_1 \end{vmatrix}=0\ . \tag{A1}$$

The definitions that have been used are

$$Q_1=\frac{1-z}{2(m+\overline{m})}\ln\left[\frac{1+m+\overline{m}}{1-m-\overline{m}}\right]\ , \tag{A2}$$

$$Q_2=\frac{1-z}{2(m-\overline{m})}\ln\left[\frac{1+m-\overline{m}}{1-m+\overline{m}}\right]\ , \tag{A3}$$

$$A_1=\frac{z}{2(1+\xi^2)}[\xi^2(l_{12}+l_{34})+l_{13}+l_{24}]\ , \tag{A4}$$

$$\overline{A}_1=\frac{z}{2(1+\xi^2)}[l_{12}+l_{34}+\xi^2(l_{13}+l_{24})]\ , \tag{A5}$$

$$A_2=\frac{z}{2(1+\xi^2)}[\xi^2(l_{12}-l_{34})+l_{13}-l_{24}]\ , \tag{A6}$$

$$\overline{A}_2=\frac{z}{2(1+\xi^2)}[l_{12}-l_{34}+\xi^2(l_{13}-l_{24})]\ , \tag{A7}$$

$$C_1=\frac{z}{2(1+\xi^2)}\xi(l_{12}-l_{34}-l_{13}+l_{24})\ , \tag{A8}$$

$$C_2=\frac{z}{2(1+\xi^2)}\xi(l_{12}+l_{34}-l_{13}-l_{24})\ , \tag{A9}$$

where ξ and l_{ij} are defined in Sec. III. Solving (A1) in combination with Eqs. (4.3)–(4.6) leads to an analytic expression for the boundary between the antiferromagnetic Ising and mixed phases.

[1]C. N. Yang and T. D. Lee, Phys. Rev. **87**, 410 (1952).
[2]M. E. Fisher, Rep. Prog. Phys. **30**, 615 (1967).
[3]T. Matsubara and H. Matsuda, Prog. Theor. Phys. **16**, 569 (1956); H. Matsuda and T. Matsubara, *ibid.* **17**, 19 (1957).
[4]R. Micnas, J. Ranninger, and S. Robaszkiewicz, Rev. Mod. Phys. **62**, 113 (1990).
[5]S. Robaszkiewicz, R. Micnas, and K. A. Chao, Phys. Rev. B **23**, 1447 (1981).
[6]M. Suzuki, in *Advances on Phase Transitions and Disorder Phenomena,* Proceedings of the international meeting held in Amalfi, Italy, June 1986, edited by G. Busiello, L. De Cesare, F. Mancini, and M. Marinaro (World Scientific, Singapore, 1987); M. Suzuki, J. Phys. Soc. Jpn. **55**, 4205 (1986); M. Suzuki, M. Katori, and X. Hu, *ibid.* **56**, 3092 (1987).
[7]I. O. Kulik and A. G. Pedan, Sov. J. Low Temp. Phys. **9**, 127 (1983).
[8]T. Morita, J. Math. Phys. **13**, 115 (1972).
[9]G. An, J. Stat. Phys. **52**, 727 (1988).
[10]G. S. Rushbrooke, G. A. Baker, Jr., and P. J. Wood, in *Phase Transitions and Critical Phenomena,* edited by C. Domb and M. S. Green (Academic, New York, 1974), Vol. 3.
[11]D. D. Betts, in *Phase Transitions and Critical Phenomena* (Ref. 10), Vol. 3; J. Rogiers, E. W. Grundke, and D. D. Betts, Can. J. Phys. **57**, 1719 (1979).
[12]C. Domb, in *Phase Transitions and Critical Phenomena* (Ref. 10), Vol. 3.
[13]R. Kikuchi, Ann. Phys. (N.Y.) **4**, 1 (1958).
[14]P. W. Kasteleyn and J. van Kranendonk, Physica **22**, 317 (1956); **22**, 367 (1956); **22**, 387 (1956).
[15]P. W. Anderson, Phys. Rev. **80**, 922 (1950).
[16]R. C. Brower, F. Kuttner, M. Nauenberg, and K. Subbarao, Phys. Rev. Lett. **38**, 1231 (1977).
[17]H. Takano and M. Suzuki, J. Stat. Phys. **26**, 635 (1981); C. Castellani, C. Di Castro, and J. Ranninger, Nucl. Phys. **B200**, [FS4], 45 (1982).